Advanced Composite Materials
Publication details, including instructions for authors and subscription information:
http://www.tandfonline.com/loi/tacm20

Torsional damping properties of an FRP laminated cylinder

L. Bao , A. Tamura , M. Sakurai , M. Nakazawa & K. Kemmochi

Version of record first published: 02 Apr 2012.

To cite this article: L. Bao , A. Tamura , M. Sakurai , M. Nakazawa & K. Kemmochi (2005): Torsional damping properties of an FRP laminated cylinder, Advanced Composite Materials, 14:3, 229-238

To link to this article: http://dx.doi.org/10.1163/1568551054922610

Adv. Composite Mater., Vol. 14, No. 3, pp. 229–238 (2005)

Also available online - www.vsppub.com

Torsional damping properties of an FRP laminated cylinder

L. BAO *, A. TAMURA, M. SAKURAI, M. NAKAZAWA and K. KEMMOCHI

Faculty of Textile Science and Technology, Shinshu University, 3-15-1 Tokida, Ueda, 386-8567, Japan

Received 3 September 2004; accepted 25 November 2004

Abstract—The dynamic characteristics of FRP are important for robotic arms and other applications. In this work, we applied a damping capacity concept to the torsional damped oscillation of a laminated composite cylinder. The forecasting method was suggested for the torsional damping characteristic. An experiment was conducted to verify the theory and this calculation method. Good agreement was obtained between the theoretical and the experimental values of seven types of laminated composite cylinder (unidirectional (0°, 90°) plies and cross-plies (±15°, ±30°, ±45°, ±60°, ±75°)). This demonstrates that the mathematical technique developed here is satisfactory for predicting the damping of laminated composite cylinders. Torsional damping characteristics of laminated composite cylinders vary with fiber orientation angle.

Keywords: Damping capacity; torsional damped oscillation; laminated composite cylinders.

1. INTRODUCTION

When a composite is used as a structural member, the damping characteristics are very important. Such composites also have better damping characteristics than metals. For example, the precision movement in a robotic arm and the silent operation of a propeller shaft in an automobile are closely related to the torsional damping properties.

There are many studies on the damping characteristics of fiber-reinforced materials. For example, Ni and Adams [1] studied, both theoretically and experimentally, the effect of fiber orientation angle on the dynamic properties of composite beams. A method employing damping capacity was proposed. Fujimoto [2, 3] examined the bending damping of a composite, which has damping material between the layers. In the bending vibration of CF/PEEK laminating materials, the relationship

*To whom correspondence should be addressed. E-mail: baolimi@giptc.Shinshu-u.ac.jp

between damping characteristics and fiber orientation angle was revealed by Aoki and Ben [4]. Willway [5] suggested a guideline of a dynamic design for composite materials, which describes the natural frequency and damping characteristics of materials based on evaluation. However, there are no studies on the torsional damping characteristics of composite materials.

This study develops an apparatus that can be used to measure the torsional damped vibration characteristic of FRP poles, to study the relationship between the fiber orientation angle and the torsional damping characteristics. We conducted simulations to observe the effect of parameters on the torsional vibration damping characteristics.

2. TORSIONAL DAMPING THEORY

Figure 1 depicts the fiber coordinate system in the k'th layer of the fiber-reinforced materials. The x- and y-axes correspond to the cylinder longitudinal direction and circumferential direction respectively. The L-axis corresponds with the fiber direction. The stress and strain in the k'th layer are as follows.

$$\begin{Bmatrix} \sigma_x \\ \sigma_y \\ \tau_{xy} \end{Bmatrix} = \begin{bmatrix} C_{11} & C_{12} & C_{16} \\ C_{12} & C_{22} & C_{26} \\ C_{16} & C_{26} & C_{66} \end{bmatrix} \begin{Bmatrix} \varepsilon_x \\ \varepsilon_y \\ \gamma_{xy} \end{Bmatrix}, \tag{1}$$

$$\begin{aligned}
&C_{11} = Q_{11}l^4 + 2(Q_{12} + 2Q_{66})l^2m^2 + Q_{22}m^4, \\
&C_{12} = Q_{12}(l^4 + m^4) + (Q_{11} + Q_{22} - 4Q_{66})l^2m^2, \\
&\cdots\cdots \\
&C_{66} = (Q_{11} + Q_{22} - 2Q_{12} - 2Q_{66})l^2m^2 + Q_{66}\left(l^4 + m^4\right), \\
&Q_{11} = \frac{E_L}{1 - \nu_{LT}\nu_{TL}}, \quad Q_{22} = \frac{E_T}{1 - \nu_{LT}\nu_{TL}}, \\
&Q_{12} = \frac{\nu_{TL}E_L}{1 - \nu_{LT}\nu_{TL}} = \frac{\nu_{LT}E_T}{1 - \nu_{LT}\nu_{TL}}, \\
&Q_{66} = G_{LT}.
\end{aligned}$$

Here, $l = \cos\theta$, $m = \sin\theta$, E_L is Young's modulus in the longitudinal direction (L), E_T is Young's modulus in transverse direction (T), G_{LT} is the shear rigidity, and ν is Poisson's ratio.

In a symmetric laminated plate, the stress resultant (N_x, N_y, N_{xy}) and strain in the k'th layer are as follows.

$$\begin{Bmatrix} N_x \\ N_y \\ N_{xy} \end{Bmatrix} = \sum_{k=1}^{n} (h_k) \begin{bmatrix} C_{11} & C_{12} & 0 \\ C_{12} & C_{22} & 0 \\ 0 & 0 & C_{66} \end{bmatrix}_k \begin{Bmatrix} \varepsilon_x \\ \varepsilon_y \\ \gamma_{xy} \end{Bmatrix}. \tag{2}$$

Here, h_k is thickness of the k'th layer.

In this study, we observe twisting of a cylinder only.

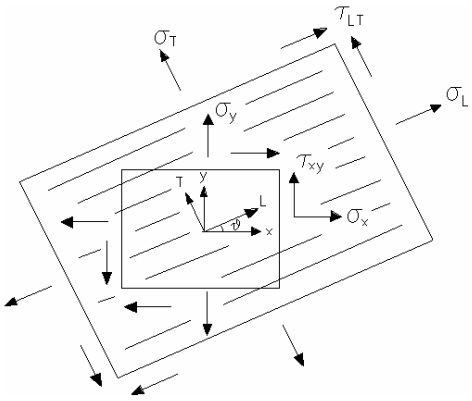

Figure 1. Fiber coordinate system.

$$\varepsilon_x = \varepsilon_y = 0, \qquad N_x = N_y = 0,\ N_{xy} = \left(\sum_{k=1}^{n} h_k C_{66}^k\right)\gamma_{xy}. \tag{3}$$

The vibration damping of the sample can be described in terms of damping capacity. In torsional vibration, the damping capacity ψ is as follows:

$$\psi = \Delta Z / Z, \tag{4}$$

where ΔZ is the energy dissipation during a stress cycle, and Z is the maximum strain energy.

$$Z = \frac{1}{2}\left(\sum_{k=1}^{n} h_k C_{66}^k\right)\gamma_{xy}^2. \tag{5}$$

The energy dissipation was divided into three separate parts, each being directly associated with the shear, longitudinal, and transverse stresses in the fiber coordinate system as follows:

$$\Delta Z^\theta = \Delta Z_L^\theta + \Delta Z_T^\theta + \Delta Z_{LT}^\theta, \tag{6}$$

where

$$\Delta Z_L^\theta = \sum_{k=1}^{n} \frac{1}{2}\sigma_L^k \varepsilon_L^k \psi_L h_k = \frac{1}{2}\psi_L \gamma_{xy}^2 \sum_{k=1}^{n} l^k m^k \left(l^{k^2} C_{16}^k + m^{k^2} C_{26}^k + 2 l^k m^k C_{66}^k\right) h_k,$$

$$\Delta Z_T^\theta = \sum_{k=1}^{n} \frac{1}{2}\sigma_T^k \varepsilon_T^k \psi_T h_k$$

$$= \frac{1}{2}\psi_T \gamma_{xy}^2 \sum_{k=1}^{n} l^k m^k \left(m^{k^2} C_{16}^k + l^{k^2} C_{26}^k - 2 l^k m^k C_{66}^k\right) h_k,$$

$$\Delta Z_{LT}^{\theta} = \frac{1}{2}\tau_{LT}^k \gamma_{LT}^k \psi_{LT} h_k$$

$$= \frac{1}{2}\psi_{LT} \gamma_{xy}^2 \sum_{k=1}^{n} \left(l^{k^2} - m^{k^2}\right)\left\{-l^k m^k C_{16}^k + l^k m^k C_{26}^k + \left(l^{k^2} - m^{k^2}\right) C_{66}^k\right\} h_k,$$

where ψ_L is the damping capacity in the longitudinal direction (L), and ψ_T is the damping capacity in the transverse direction (T), in prepreg material. They can be obtained by the bending vibration test of 0° and 90° samples. ψ_{LT} is the damping capacity in the LT direction and can be obtained by the torsional vibration test of 0 and 90° samples.

The vibration damping properties of the sample can be described as follows.

$$\psi^{\theta} = \psi_L^{\theta} + \psi_T^{\theta} + \psi_{LT}^{\theta}, \tag{7}$$

$$\psi_L^{\theta} = \frac{\Delta Z_L}{Z} = \frac{\psi_L}{A_{66}} \sum_{k=1}^{n} l^k m^k \left(l^{k^2} C_{16}^k + m^{k^2} C_{26}^k + 2 l^k m^k C_{66}^k\right) h_k,$$

$$\psi_T^{\theta} = \frac{\Delta Z_T}{Z} = -\frac{\psi_T}{A_{66}} \sum_{k=1}^{n} l^k m^k \left(m^{k^2} C_{16}^k + l^{k^2} C_{26}^k - 2 l^k m^k C_{66}^k\right) h_k,$$

$$\psi_{LT}^{\theta} = \frac{\Delta Z_{LT}}{Z} = \frac{\psi_{LT}}{A_{66}} \sum_{k=1}^{n} \left(l^{k^2} - m^{k^2}\right)\left\{-l^k m^k C_{16}^k + l^k m^k C_{26}^k + \left(l^{k^2} - m^{k^2}\right) C_{66}^k\right\} h_k.$$

3. EXPERIMENTAL PROCEDURE

The schematic diagram of the experiment equipment is illustrated in Fig. 2. The upper end of the specimen was fixed by a vice, and lower end, by a large sink for the inertia moment. The specimen was twisted by pulling symmetrically in a specific direction, thus applying constant distortion. The specimen opens momentarily and torsional vibration is generated. The curve (Figs 3 and 4) of the damped oscillation is obtained from the outputs of strain gages, which were pasted onto the specimen. The relationship between the logarithmic decrement δ and ψ is

$$\delta = \ln \frac{A_i}{A_{i+1}}, \quad \xi = \frac{\delta^2}{\sqrt{(2\pi)^2 + \delta^2}}. \tag{8}$$

The damping capacity of the specimen is as follows.

$$\psi = 4\pi\xi. \tag{9}$$

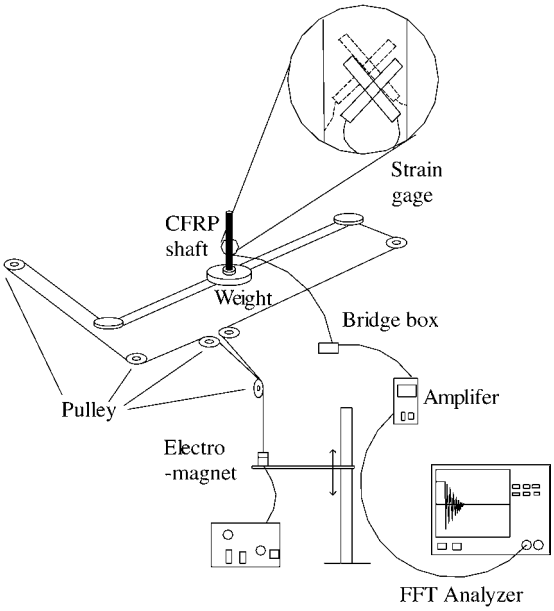

Figure 2. Test apparatus for torsional damping.

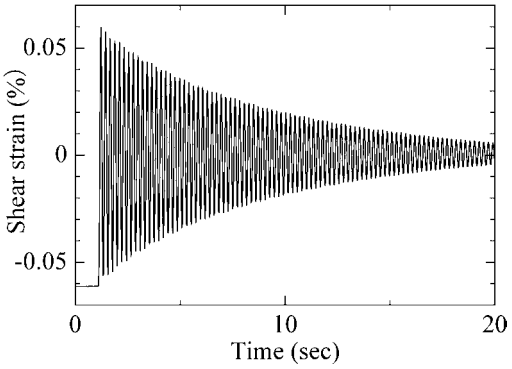

Figure 3. Waveform of torsional damping for sample CFRP 15°.

Young's modulus (E_L, E_T), and Poisson's ratio (ν_{LT}) of samples analyzed were obtained by tensile tests (Simadzu Co., Ltd., AG20KND). We used 0 and 90 degree materials as specimens and tested them five times at a speed of 0.05 /s.

The shear rigidity of samples was obtained by a torsional test (Simadzu Co. Ltd., AG20KND and CM22-2028). They were tested three times at a speed of 0.01/s. The axis force was controlled at 1.0 N for pure torsional testing.

Properties of all the fabric samples are displayed in Table 1. The fiber orientation angles are 0°, 15°, 30°, 45°, 60°, 75°, and 90°. The samples are 8-layer angle-ply, with sizes depicted in Fig. 5.

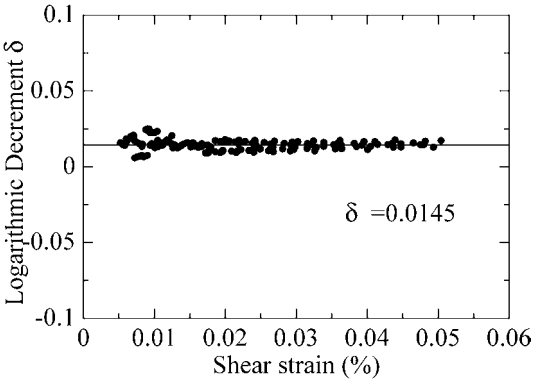

Figure 4. Relationship between shear strain and logarithmic decrement for sample CFRP 15°.

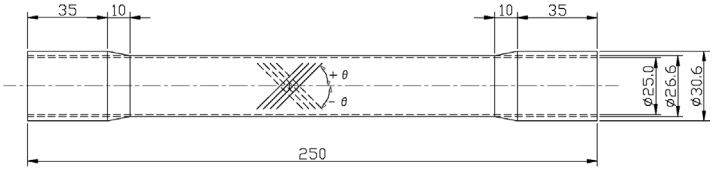

Figure 5. Specimen diagram.

Table 1.
Specimen details

	CFRP	AFRP
Fiber	Carbon fiber (Mitsubishi Rayon Co., Ltd.)	Vectran fiber (Kuraray Co., Ltd.)
Resins	Epoxy resin	
Prepreg	TR350E–100	AFUD-PPHS-100
Fiber orientation angle	0°, ±15°, ±30°, ±45°, ±60°, ±75°, 90°	
Condition of lay-up	Circular cylinder is made form lamina (laminated $(\pm\theta)_{4s}$)	
E_L (GPa)	133.28	45.15
E_T (GPa)	8.35	3.34
ν_{LT}	0.323	0.470
ν_{LT}	0.022	0.011
G_{LT} (MPa)	3.70	1.20

4. RESULTS AND DISCUSSION

We converted a curve (measured as in Fig. 4 with an experimental device with torsional damping) into damping capacity. Figure 6 indicates the experiment results (CFRP laminated cylinder; fiber orientation angle 0, 15, 30, 45, 75, and 90). It illustrates the relationship between fiber orientation angle and damping capacity of

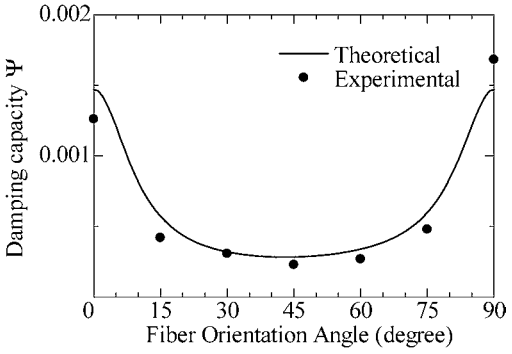

Figure 6. Relationship between fiber orientation and damping capacity of CFRP.

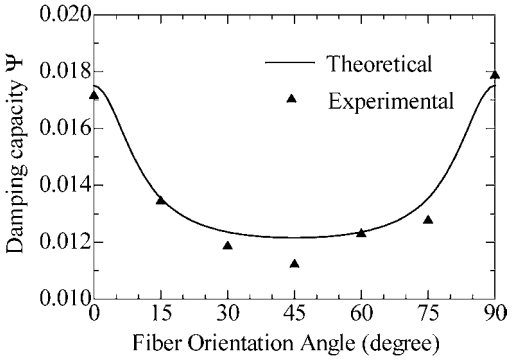

Figure 7. Relationship between fiber orientation and damping capacity of AFRP.

CFRP. The dot represents experiment values. The damping capacity is the minimum value with the 45° material. The others are approximately symmetrical values at 45°. The figure indicates that damping capacity of CFRP laminated structure is mainly influenced by the fiber orientation angle 0° and 90° are materials with the greatest damping capacities.

The line in Fig. 6 is the result calculated using the data of Table 1 and equation (7). There is good agreement between the experimental and theoretical values.

Figure 7 illustrates the relationship between fiber orientation and the damping capacity of AFRP. There is also good agreement between the experimental and theoretical values. The tendency in variations of the two materials also agrees. However, AFRP exhibits the greatest torsional damping.

Thus, applicability of the formula suggested in this research was confirmed.

Using the data of Table 1 and equation (7), we conducted simulations to observe how the parameters affect the torsional damping capacity of FRP. Figures 8 and 9 are the results of simulations. In Fig. 8, we increased E_L by 2, 4, 8, and 16 times then reduced it by 1/2, 1/4, 1/8 and 1/16 while keeping the other parameters ($E_T, G_{LT}, \psi_L, \psi_T, \psi_{LT}$) constant, illustrating that torsional damping capacity decreased as E_L increased. E_L affects the values of the torsional damping

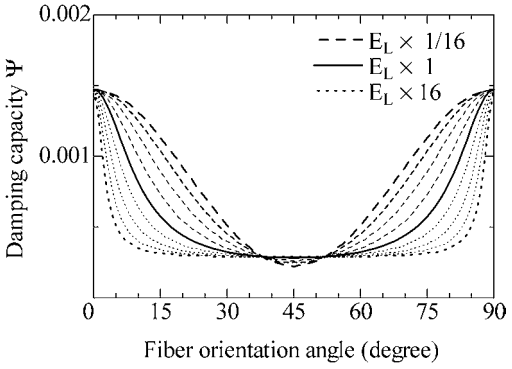

Figure 8. Relationship between fiber orientation angle and damping capacity for various values of E_L.

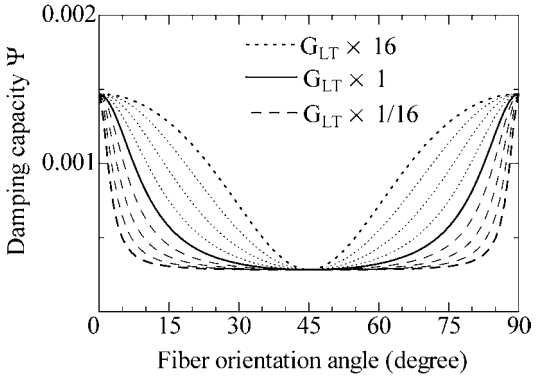

Figure 9. Relationship between fiber orientation angle and damping capacity for various values of G_{LT}.

capacity greatly at 0 and 90 degrees. E_T has little effect compared with E_L on the torsional damping capacity.

In Fig. 9, we increased G_{LT} by 2, 4, 8, and 16 times then reduced it by $1/2$, $1/4$, $1/8$ and $1/16$ while keeping the other parameters (E_L, E_T, ψ_L, ψ_T, ψ_{LT}) constant. We observed that torsional damping capacity increased as G_{LT} increased. The G_{LT} effects on the values of the torsional damping capacity are great at 0 and 90 degrees. This result is opposite to the results obtained from Fig. 8. Both figures are perfectly symmetric.

Damping capacities (ψ_L, ψ_T, ψ_{LT}) are damping properties of the prepreg materials. We increased ψ_L by 2, 4, 8, and 16 times then reduced it by $1/2$, $1/4$, $1/8$ and $1/16$ while keeping the other parameters (E_L, E_T, G_{LT}, ψ_T, ψ_{LT}) constant. We observed that torsional damping capacity increased as ψ_L increased (Fig. 10). We also observed that ψ_L affects the torsional damping capacity greatly at 45 degrees. Torsional damping capacity increased as ψ_{LT} increased (Fig. 11). ψ_{LT} affects the torsional damping capacity greatly at 0 and 90 degrees. The effect of ψ_{LT} is largest in seven basic parameters.

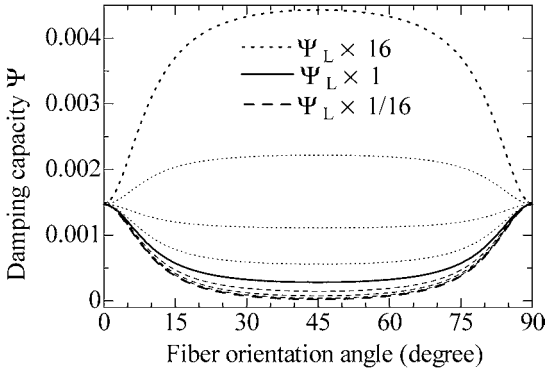

Figure 10. Relationship between fiber orientation angle and damping capacity for various values of ψ_L.

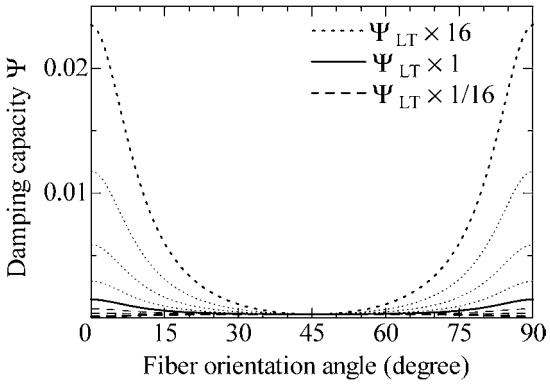

Figure 11. Relationship between fiber orientation angle and damping capacity for various values of ψ_{LT}.

5. CONCLUSIONS

We developed an apparatus that can be used to measure the torsional damped vibration characteristics of FRP poles in order to study the relationship between the fiber orientation angle and the torsional damping characteristics. We also conducted simulations to see how the parameters affect the torsional damping vibration characteristics.

1. Good agreement was obtained between the theoretical and the experimental values in torsional damping capacity.
2. The experimental values indicate that torsional damping capacity is minimum when the fiber orientation angle is 45 degrees, and the other values increase almost symmetrically as the orientation angles deviate from 45 degrees.
3. E_L, G_{LT}, ψ_L, and ψ_{LT} of prepreg materials greatly affect torsional damping capacity. E_T has little effect.

Acknowledgements

This work was supported by a Grant-in-Aid for COE Research (10CE2003) and Scientific Research (C)(2) 13650081 by the Ministry of Education, Culture, Sports, Science and Technology of Japan.

REFERENCES

1. R. Ni and R. Adams, *J. Compos. Materials* **18**, 104–121 (1984).
2. J. Fujimoto and T. Tamura, *J. Jpn Soc. Compos. Mater.* **20**, 145–153 (1994).
3. J. Fujimoto and T. Tamura, *J. Jpn Soc. Compos. Mater.* **20**, 154–161 (1994).
4. Y. Aoki, G. Ben and K. Kasumi, *Materials* **41**, 1121–1125 (1992).
5. T. A. Willway and R. G. White, *Compos. Sci. Technol.* **36**, 77–94 (1989).